Article

The Comparative Investigation of Corrosion and Passivation for X65 Carbon Steel in pH 1 to 5 HNO$_3$ Solutions without and with 0.01 mol L^{-1} NaNO$_2$

Rongjiao Deng,[a] Pei Zhang,[b] Xiaoying Zhao,[a] Guanyu Cai,[a] Hui Liu,[a] Jinping Xiong ✱,[a] and Yong Zhou ✱,[c]

[a]State Key Laboratory of Chemical Resource Engineering,
Beijing Key Laboratory of Electrochemical Process and Technology for Materials,
Beijing University of Chemical Technology, 100029 Beijing, China

[b]College of Chemistry and Food Science,
Guangxi Key Laboratory of Agricultural Resources Chemistry and Biotechnology,
Yulin Normal University, 537000 Yulin, China

[c]Key Laboratory for Green Chemical Process of Ministry of Education,
Hubei Key Laboratory of Novel Reactor and Green Chemical Technology,
Wuhan Institute of Technology, 430205 Wuhan, China

The influence of 0.01 mol L^{-1} NaNO$_2$ addition on the corrosion and passivation of X65 carbon steel in pH 1 to 5 HNO$_3$ solutions was investigated and compared by electrochemical methods and microstructural techniques. In the pH 1 to 5 solutions without NaNO$_2$, the X65 steel presented the electrochemical characteristic of active dissolution, and the corrosion rate of X65 carbon steel decreased gradually with the raise of pH value. By contrast, with the addition of 0.01 mol L^{-1} NaNO$_2$ in pH 1 to 5 HNO$_3$ solutions, the electrochemical characteristic of X65 carbon steel transferred from the active dissolution in the pH 1 to 5 solutions without NaNO$_2$ to the anodic passivation in the corresponding pH solutions with NaNO$_2$. For the X65 steel in the pH 1 to 5 solutions with NaNO$_2$, with the raise of pH value, the corrosion rate also decreased gradually but the passivation capability strengthened obviously. The corrosion and passivation of X65 carbon steel in pH 1 to 5 HNO$_3$ solutions without and with 0.01 mol L^{-1} NaNO$_2$ were related to the cathodic reactions of H$^+$ reduction, O$_2$ reduction and NO$_2^-$/HNO$_2$ reduction.

Keywords: X65 carbon steel, HNO$_3$, NaNO$_2$, corrosion, passivation, electrochemical

Introduction

The application of carbon steels in production and living fields is wide and universal;[1-3] however, the inevitability of corrosion and failure usually leads to the untimely damage of steel structure.[4-6] The addition of inhibitors into environmental media is the one of main and important methods to decrease the corrosion rate of carbon steels in their service condition,[7] which is attributed to the oxidation or the adsorption mechanism of inhibitors on the surface of carbon steels.[8] NO$_2^-$ is a kind of oxidation-type inhibitor[9] and can promote the surface passivation of carbon steels due to the formation of surface passive film.[10-12]

In alkaline and neutral environments, the related reports involving the passivation function of NO$_2^-$ on the steel surface have been published repeatedly.[13-18] Lee *et al.*,[13] Dong *et al.*,[14,15] Valcarce and Vazquez[16] and Reffass *et al.*[17] respectively reported the effectiveness of NO$_2^-$ on the surface passivation of carbon steels in synthetic tap water (pH 7.2), in simulated carbonated concrete pore solution (pH 12.0), in mixed alkaline solution containing Cl$^-$ (pH 13.9) and in mixed NaHCO$_3$ and NaCl solution (pH 8.3). The addition of NO$_2^-$ into the above environmental media promoted the repassivation on the steel surface, and the mechanism of NO$_2^-$ was mainly due to the following reaction:[13]

$$2Fe^{2+} + 2OH^- + 2NO_2^- \rightarrow 2NO + \gamma\text{-}Fe_2O_3 + H_2O \qquad (1)$$

For the natural passive film on the surface of carbon steels formed in atmosphere, γ-Fe$_2$O$_3$ repaired the defects in the film interiors[14] and made the film rearrange a regular microstructure.[17]

*e-mail: xiongjp@mail.buct.edu.cn; zhouyong@wit.edu.cn

However, for the surface passivation of carbon steels in acidic environments, the effectiveness of NO_2^- is very few reported, and the detailed mechanism of NO_2^- is still not completely clear. Zhou *et al.*[19-21] systemically investigated the influences of $NaNO_2$ addition and its concentration on the corrosion and passivation of Q235 carbon steel in CO_2 saturated solution (pH 3.7). The electrochemical behavior of Q235 carbon steel transferred from the activation in CO_2 saturated solution free of $NaNO_2$ to the passivation in the same solution containing $NaNO_2$;[19] with the increase of $NaNO_2$ concentration, the passivation capability of Q235 carbon steel was strengthened obviously until the $NaNO_2$ concentration was up to 0.05 mol L^{-1};[20] the mechanism of NO_2^- on the surface passivation was very closely associated with the formation of Fe_2O_3 passive film under $FeCO_3$ corrosion product layer.[21] Further, Zhou *et al.*[22] also investigated the influence of $NaNO_2$ addition on the electrochemical behavior of Q235 carbon steel in pH 1 to 6 HCl solutions. Due to the absence of strong oxidability and the presence of Cl^- in HCl solutions, the effectiveness of $NaNO_2$ on the surface passivation was very limited, and the occurrence of pitting corrosion was present when a high potential was applied. Besides, Zuo *et al.*[23] and Garces *et al.*[24] reported the influences of $NaNO_2$ on the corrosion and passivation for the X70 steel in acidic NaCl solution (pH 5.5) and for the corrugated steel bar in simulated pit solution (pH 1.46 to 6.38), respectively. Nevertheless, at present, the related mechanism of NO_2^- on the surface passivation of carbon steels in acidic environments still needs to be further studied.

As summarized above, until by now, the reports involving the effectiveness of NO_2^- on the surface passivation of carbon steels in CO_2 saturated solution (a weak and non-oxidizing acid environment)[20] and in pH 1 to 6 HCl solutions (a strong and non-oxidizing acid environment)[22] have been published. However, in strong and oxidizing acid environments, such as HNO_3 solutions, the related investigations are absent. Therefore, in this work, 0.01 mol L^{-1} $NaNO_2$ is added in pH 1 to 5 HNO_3 solutions, and the electrochemical methods of open circuit potential (OCP) evolution, potentiodynamic polarization curve and electrochemical impedance spectroscopy (EIS) are carried out to investigate and compare the corrosion and passivation of X65 carbon steel in pH 1 to 5 HNO_3 solutions without and with 0.01 mol L^{-1} $NaNO_2$.

Experimental

The investigated material was X65 carbon steel with the following chemical composition (wt.%): C, 0.030; Si, 0.170; Mn, 1.510; P, 0.024; S, 0.005; Mo, 0.160; Ni, 0.170; Cu, 0.040; Al, 0.020; Ti, 0.010; N, 0.006;

Nb, 0.060; Fe, balance. Samples were manually abraded up to 1000 grit with SiC abrasive papers, rinsed with de-ionized water and degreased in alcohol.

The investigated solutions were pH 1 to 5 HNO_3 solutions without and with the addition of 0.01 mol L^{-1} $NaNO_2$. After adding $NaNO_2$, the pH value of each solution was adjusted with the introduction of diluted HNO_3.

The electrochemical measurements of OCP evolution, potentiodynamic polarization curve and EIS were conducted using a CS310 electrochemical workstation (Wuhan Corrtest Instruments Corp., Ltd, China). A typical three electrode system was applied for all the electrochemical measurements. The system was composed of a saturated calomel electrode (SCE) as reference electrode (RE), a platinum sheet as counter electrode (CE) and an X65 sample as working electrode (WE). The sizes of CE and WE were 1.0×1.0 cm and 0.2×0.2 cm, respectively; WE was polished once again after each electrochemical test. According to the results of OCP evolution, the WE was immersed in the corresponding investigated solution for 10 min before the electrochemical tests of polarization and EIS were begun. In the OCP test, the recording frequency of potential was 5 Hz. In the polarization test, the potential scanning rate was 0.5 mV s^{-1}, and the potential scanning range was from $-0.2\,V_{OCP}$ to the potential value corresponding to the objective electrochemical characteristic. In the EIS test, a perturbation potential of 10 mV amplitude was applied in the frequency range from 10^5 to 10^{-2} Hz. The schematic diagram of electrochemical testing system was shown in Figure 1. All electrochemical measurements were performed at 25 °C, which was controlled with an electro-thermostatic water bath.
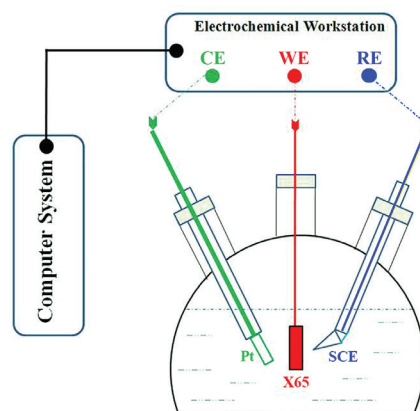

Figure 1. Schematic diagram of electrochemical testing system.

The surface morphologies were observed by an SU1510 scanning electron microscope (SEM) instrument (Hitachi High-Technologies Corporation, Japan), and the surface composition was detected by a Kevex SuperDry energy

dispersion X-ray spectroscopy (EDS) instrument attached on the SEM system.

Results and Discussion

Figure 2 shows the OCP evolutions and the potentiodynamic polarization curves of X65 samples in pH 1 to 5 HNO_3 solutions without 0.01 mol L^{-1} $NaNO_2$. From Figure 2a, in the different pH solutions, OCP stabilizes gradually with the extensive immersion time and shows the stable value when the immersion time is up to 10 min. Therefore, in the following electrochemical tests of polarization and EIS, all the X65 samples were immersed in the corresponding solutions for 10 min before the polarization and EIS tests were begun.

In the pH 1 to 3 solutions without $NaNO_2$, the stable OCP value decreases with the raise of pH value, as shown in Figure 2a. Similar result is also observed on the potentiodynamic polarization curves shown in Figure 2b: corrosion potential (E_{corr}) moves to the negative direction with the raise of pH value from 1 to 3. The above influences of pH values on OCP and E_{corr} suggest that the dominated cathodic reaction occurred on the X65 surface in the pH 1 to 3 solutions without $NaNO_2$ is the H^+ reduction with the standard potential (E_{st}) of 0 V_{SHE} (SHE: standard hydrogen electrode):

$$2H^+ + 2e \rightarrow H_2 \ (E_{st} = 0 \ V_{SHE}, \ pH \ 0) \tag{2}$$

In very acidic environments, the influence of pH value on the equilibrium potential (E_{eq}) of H^+ reduction (equation 2) can be described as follows:[25]

$$E_{eq} \ (H^+/H_2) = -0.059 \ pH \tag{3}$$
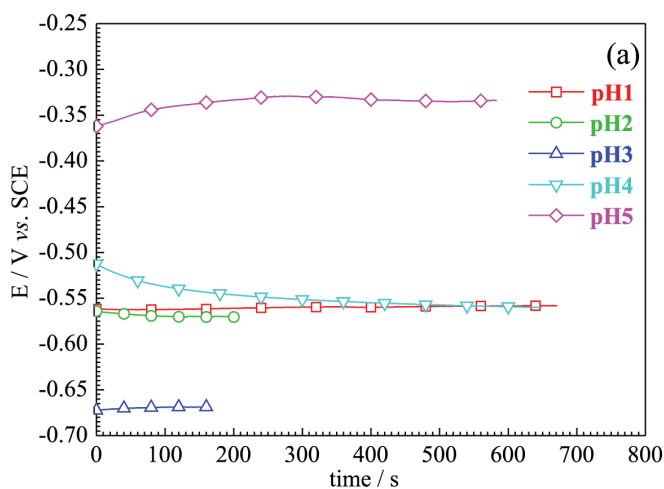
In the pH 1 to 3 solutions without $NaNO_2$, with the raise of pH value, the E_{eq} (H^+/H_2) value decreases, so the stable OCP and the E_{corr} move to the negative direction.
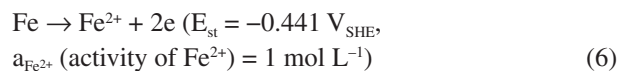
Further, in the pH 3 to 5 solutions without $NaNO_2$, the stable OCP and the E_{corr} move to the positive direction with the raise of pH value. From Figure 2b, on the one hand, the value of corrosion current density (i_{corr}) for the X65 steel in the pH 4 to 5 solutions without $NaNO_2$ are in the order of magnitudes between 10^{-6} and 10^{-5} A cm^{-2}. On the other hand, the corrosion rate of X65 carbon steel in the pH 4 to 5 solutions is obvious lower than that in the pH 1 to 3 solutions. The above two aspects suggest that the O_2 reduction has become the dominated cathodic reaction occurred on the X65 surface in the pH 4 to 5 solutions without $NaNO_2$:
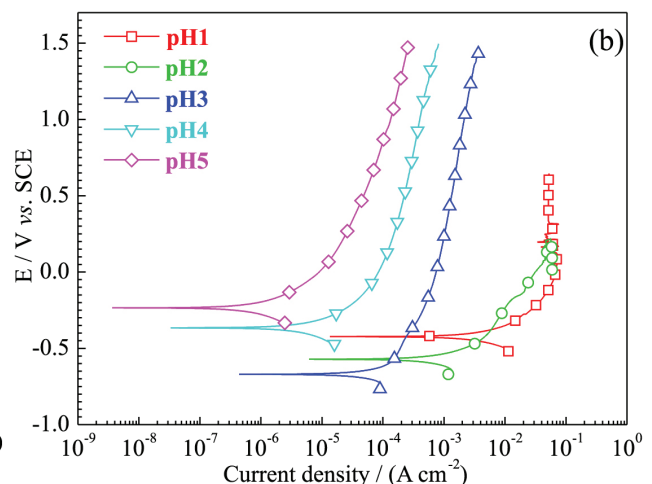
$$O_2 + 2H_2O + 4e \rightarrow 4OH^- \ (E_{st} = 1.220 \ V_{SHE}, \ pH \ 0) \tag{4}$$
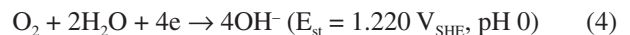
At the same time, the influence of pH value on the E_{eq} of O_2 reduction (equation 4) can be described as follows:[25]

$$E_{eq} \ (O_2/OH^-) = 1.228 - 0.059 \ pH \tag{5}$$

In the pH 4 to 5 solutions without $NaNO_2$, the stable OCP and the E_{corr} move to the positive direction with the raise of pH value, which may be attributed to the influences of pH values on the electrode reactions of O_2 reduction and Fe oxidation. The Fe oxidation is the main anodic reaction occurred on the surface of carbon steels in acidic environments:

$$Fe \rightarrow Fe^{2+} + 2e \ (E_{st} = -0.441 \ V_{SHE},$$
$$a_{Fe^{2+}} \ (activity \ of \ Fe^{2+}) = 1 \ mol \ L^{-1}) \tag{6}$$

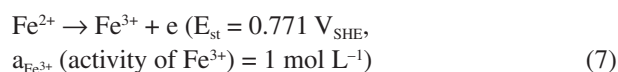In addition, from Figure 2b, for the X65 steel in the

Figure 2. OCP evolutions and potentiodynamic polarization curves of X65 samples in pH 1 to 5 HNO_3 solutions without 0.01 mol L^{-1} $NaNO_2$: (a) OCP and (b) polarization.

pH 1 to 5 solutions without $NaNO_2$, the anodic current density continuously increased with the positive shift of applied potential, indicating the electrochemical characteristic of active dissolution. It is prominent for the influence of pH value on the corrosion rate of X65 carbon steel: the i_{corr} value decreases obviously with the raise of pH value. This rule can be explained as follows. It is assumed that there is no influence of pH value on the anodic reaction of Fe oxidation (equation 6). With the raise of pH value, the chemical equilibrium of H^+ reduction (equation 2) and O_2 reduction (equation 4) will move to the left direction: the higher pH value, the stronger is the movement. The cathodic reactions are restrained, resulting in the i_{corr} decrease. However, from Figure 2b, it is noteworthy that the increasing rate of anodic current density with the applied potential is not prominent, particularly that in the pH 3 to 5 solutions, suggesting the deposition and protection of corrosion product on the surface of X65 carbon steel. Figure 3 shows the surface SEM morphologies of X65 samples polarized to $0.5\ V_{SCE}$ in the pH 3 HNO_3 solution without $0.01\ mol\ L^{-1}\ NaNO_2$. From the low-magnification SEM morphology shown in Figure 3a, corrosion product is present on the sample surface and is composed of Fe, N and O by EDS analysis. Further, from the high-magnification SEM morphology shown in Figure 3b, the presence of cracks and pores is observed on the corrosion product, indicating the limited protection for the X65 substrate. The surface SEM morphologies of X65 samples in the other four solutions are similar to those in the pH 3 solution without $NaNO_2$.
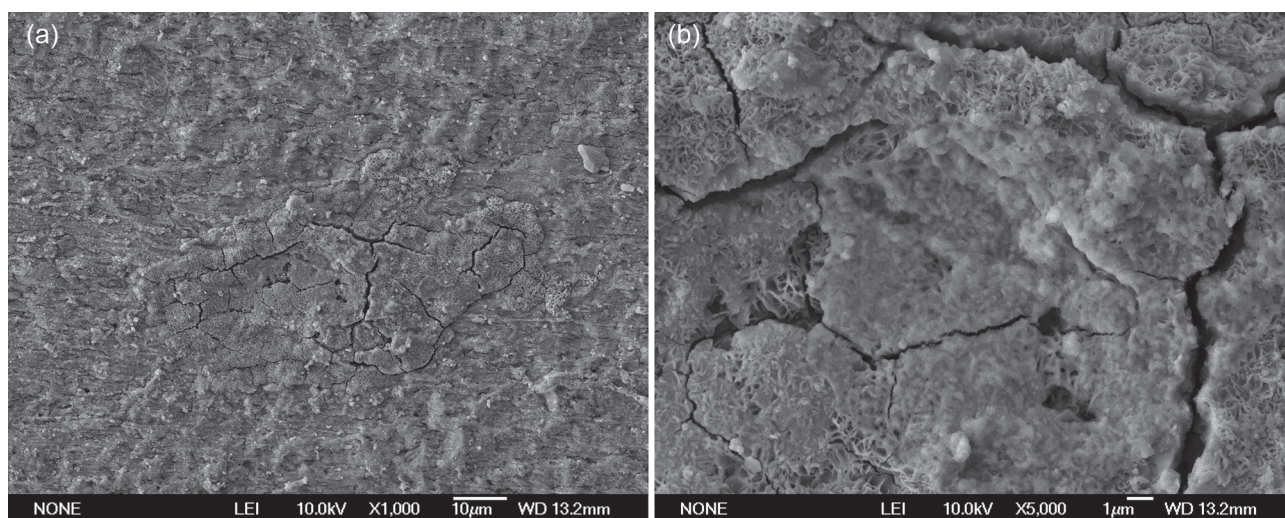
Figure 4 shows the OCP evolutions and the potentiodynamic polarization curves of X65 samples in pH 1 to 5 HNO_3 solutions with $0.01\ mol\ L^{-1}\ NaNO_2$. Comparing Figure 4b with Figure 2b, the influence of $0.01\ mol\ L^{-1}\ NaNO_2$ addition on the electrochemical

behavior of X65 carbon steel in pH 1 to 5 HNO_3 solutions is very prominent. In the pH 1 to 4 solutions with $NaNO_2$, the X65 steel presented the electrochemical characteristic of anodic passivation, and the active region, the active-passive transition region, the passive region and the transpassive region can be observed on the four polarization curves; in contrast, in the pH 5 solution with $NaNO_2$, the X65 steel presented the electrochemical characteristic of self-passivation. With the addition of $0.01\ mol\ L^{-1}\ NaNO_2$ in pH 1 to 5 HNO_3 solutions, the obvious variation of electrochemical characteristic indicates the effectiveness of NO_2^- on the surface passivation of X65 carbon steel.

For the X65 steel, when the applied potential is at the vicinity of OCP, the influences of pH values on E_{corr} and i_{corr} in the pH 1 to 5 solutions with $NaNO_2$ are similar to those in the corresponding pH solutions without $NaNO_2$, which has been explained in the previous discussion. At the same time, by SEM observation, corrosion product is also present on the surface of X65 carbon steel when the X65 steel was polarized to the active-passive transition potential (E_{trans}) in the pH 1 to 5 solutions with $NaNO_2$. However, with the positive shift of applied potential, the passive region is present on the polarization curves, as shown in Figure 4b. It is generally accepted and confirmed that the surface passivation of carbon steels is very closely related to the generation of Fe^{3+}, which is the main component of surface passive film.[13-17] Therefore, the anodic reaction of Fe^{2+} oxidation is essential for the passivation of X65 carbon steel:

$$Fe^{2+} \rightarrow Fe^{3+} + e\ (E_{st} = 0.771\ V_{SHE},$$
$$a_{Fe^{3+}}\ (activity\ of\ Fe^{3+}) = 1\ mol\ L^{-1}) \qquad (7)$$

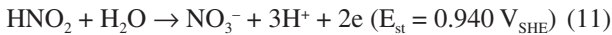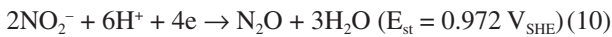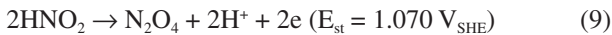However, the E_{st} of Fe^{2+} oxidation (equation 7) is more greatly positive than that of H^+ reduction (equation 2) or O_2

Figure 3. Surface SEM morphologies of X65 samples polarized to $0.5\ V_{SCE}$ in pH 3 HNO_3 solutions without $0.01\ mol\ L^{-1}\ NaNO_2$.
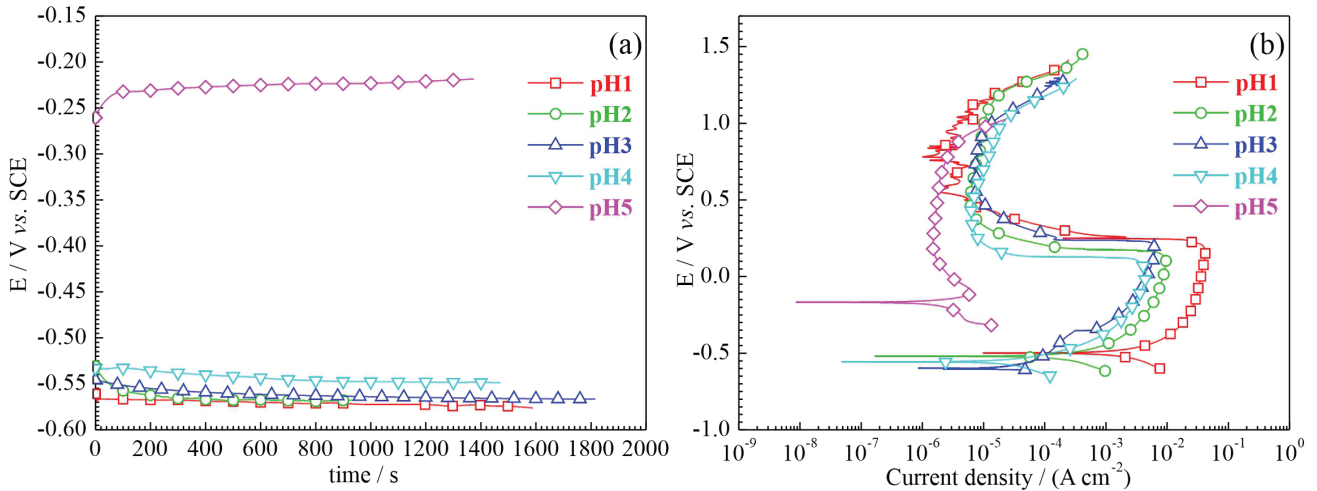
Figure 4. OCP evolutions and potentiodynamic polarization curves of X65 samples in pH 1 to 5 HNO$_3$ solutions with 0.01 mol L^{-1} NaNO$_2$: (a) OCP and (b) polarization.

reduction (equation 4), resulting in the absence of surface passivation for the X65 steel in pH 1 to 5 HNO$_3$ solutions without 0.01 mol L^{-1} NaNO$_2$.

With the addition of 0.01 mol L^{-1} NaNO$_2$ in pH 1 to 5 HNO$_3$ solutions, the presence of NO$_2^-$ makes the following cathodic reactions available:[26-28]

$$2NO_2^- + 8H^+ + 6e \rightarrow N_2 + 4H_2O \ (E_{st} = 1.188 \ V_{SHE}) \quad (8)$$
$$2HNO_2 \rightarrow N_2O_4 + 2H^+ + 2e \ (E_{st} = 1.070 \ V_{SHE}) \quad (9)$$
$$2NO_2^- + 6H^+ + 4e \rightarrow N_2O + 3H_2O \ (E_{st} = 0.972 \ V_{SHE}) (10)$$
$$HNO_2 + H_2O \rightarrow NO_3^- + 3H^+ + 2e \ (E_{st} = 0.940 \ V_{SHE}) \ (11)$$

Because the E_{st} of above reduction reaction concerning NO$_2^-$/HNO$_2$ (equation 8 to 11) is more positive than that of Fe^{2+} oxidation (equation 7), the anodic reaction of Fe^{2+} oxidation (equation 7) is possible if one or more of equations 8 to 11 occur on the X65 surface when a high potential was applied. However, the kinetic investigations and the E_{eq} calculations are necessary to verify the real cathodic reactions of NO$_2^-$/HNO$_2$ reduction, which will be carried out in the future investigations. In this work, the effectiveness of NO$_2^-$ on the surface passivation of X65

carbon steel in pH 1 to 5 HNO$_3$ solutions is certain, which can provide a degree of theoretical basis to the engineering application, similar to that of anodic protection.

Further, from Figures 2b and 4b, the influences of NaNO$_2$ addition and pH value on the corrosion and passivation parameters, including E_{corr}, i_{corr}, E_{trans}, critical passive current density (i_{crit}) and maintaining passive current density (i_{main}), are very obvious. In this work, the CVIEW software was applied to analyze the results of potentiodynamic polarization curve. Table 1 lists the calculated results of E_{corr}, i_{corr}, E_{trans}, i_{crit} and i_{main}.

It is similar the influences of pH values on E_{corr} and i_{corr} both in the pH 1 to 5 solutions without and with NaNO$_2$, which has been explained in the previous discussion. In the pH 1 to 4 solutions with NaNO$_2$, the X65 steel presented the electrochemical characteristic of anodic passivation, and it is worth noting that both the E_{trans} and i_{crit} values decrease obviously with the raise of pH value, indicating that the surface passivation in the high pH solutions is easier than that in the low pH solutions. Further, this result also suggests the cathodic reactions of equations 9 and 11 are more possible than those of equations 8 and 10. In the pH 5 solution

Table 1. Calculated results of E_{corr}, i_{corr}, E_{trans}, i_{crit} and i_{main} from the CVIEW software

pH	Without NaNO$_2$		With NaNO$_2$				
	E_{corr} / V$_{SCE}$	i_{corr} / (A cm^{-2})	E_{corr} / V$_{SCE}$	i_{corr} / (A cm^{-2})	E_{trans} / V$_{SCE}$	i_{crti} / (A cm^{-2})	i_{main} / (A cm^{-2})
1	−0.42	3.27×10^{-2}	−0.50	3.78×10^{-2}	0.17	4.17×10^{-2}	6.19×10^{-6}
2	−0.57	2.52×10^{-3}	−0.52	2.76×10^{-3}	0.10	9.58×10^{-3}	6.27×10^{-6}
3	−0.67	3.75×10^{-4}	−0.60	9.64×10^{-4}	0.16	6.31×10^{-3}	6.31×10^{-6}
4	−0.37	6.59×10^{-5}	−0.56	8.59×10^{-4}	0.01	4.50×10^{-3}	6.33×10^{-6}
5	−0.23	1.30×10^{-5}	−0.17	6.18×10^{-6}	–	–	1.48×10^{-6}

E_{corr}: corrosion potential; i_{corr}: corrosion current density; E_{trans}: active-passive transition potential; i_{crit}: critical passive current density; i_{main}: maintaining passive current density.
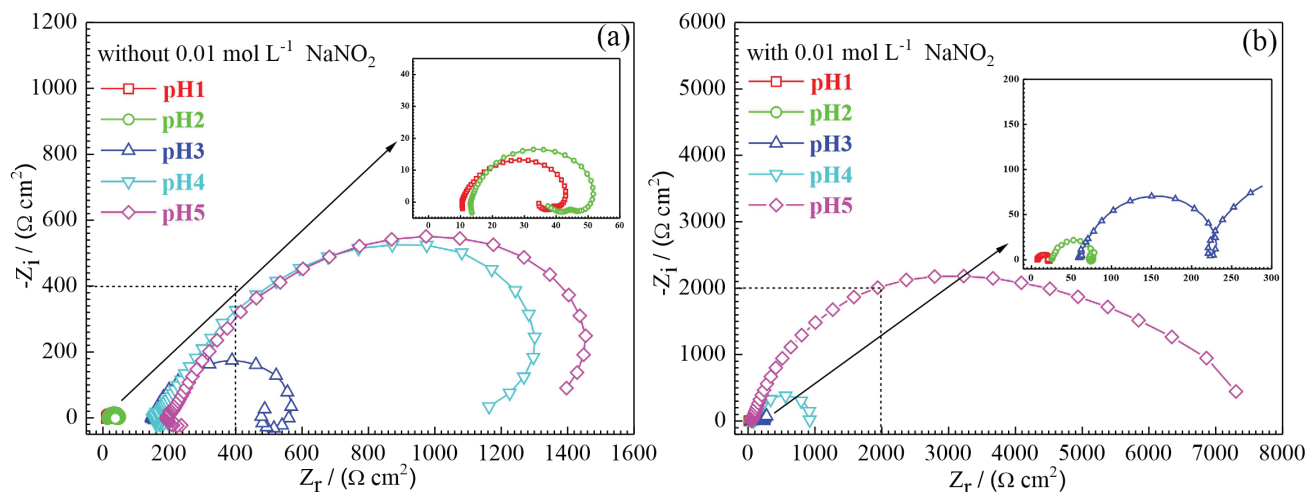
Figure 5. EIS of X65 samples in pH 1 to 5 HNO$_3$ solutions: (a) without 0.01 mol L^{-1} NaNO$_2$ and (b) with 0.01 mol L^{-1} NaNO$_2$.

with NaNO$_2$, the X65 steel presented the electrochemical characteristic of self-passivation, and the absence of active-passive transition suggests the relatively high passivation capability. Besides, the influence of pH value on the i_{main} value is not obvious in the pH 1 to 5 solutions with NaNO$_2$.

At the same time, from Table 1, the i_{corr} value in the pH 1 to 4 solutions with NaNO$_2$ is greater than that in the corresponding pH solutions without NaNO$_2$, which is also due to the presence of NO$_2^-$.[20]

Figure 5 shows the EIS of X65 samples in pH 1 to 5 HNO$_3$ solutions without and with 0.01 mol L^{-1} NaNO$_2$ at the stable OCP value. From Figure 5, the influence of 0.01 mol L^{-1} NaNO$_2$ addition on the EIS characteristic of X65 carbon steel in pH 1 to 5 HNO$_3$ solutions is also remarkable.

In the pH 1 to 3 solutions without NaNO$_2$, the three Nyquist plots are composed of two capacitive semicircles at the high frequency zone and an inductive semicircle at the low frequency zone. However, in the pH 4 to 5 solutions without NaNO$_2$, the presence of two capacitive semicircles and the absence of inductive semicircle are observed on the two Nyquist plots. From the previous discussion, for the two capacitive semicircles, one is attributed to the deposition of corrosion product on the X65 surface and the other one is due to the process of charge transfer between double electron layer;[29] the presence of inductive semicircle is attributed to the adsorption relaxation process of H$^+$,[20] and the disappearance of inductive semicircle further confirms the different cathodic reaction: H$^+$ reduction (equation 2) in the pH 1 to 3 solutions without NaNO$_2$ and O$_2$ reduction (equation 4) in the pH 4 to 5 solutions without NaNO$_2$. From Figure 5a, the radius of capacitive semicircle enlarges significantly with the raise of pH value, indicating the decrease of corrosion rate. In the pH 1 to 5 solutions with NaNO$_2$, the five Nyquist plots are composed

of two capacitive semicircles at the entire frequency zone, which is also due to the deposition of corrosion product and the charge transfer between double electron layer. From Figure 5b, the radius of capacitive semicircle also enlarges with the raise of pH value.

Further, the method of equivalent electrical circuit (EEC) interpretation is applied to fit the EIS results. For the EIS obtained in the pH 1 to 3 solutions without NaNO$_2$, two capacitive semicircles and an inductive semicircle are present, so the EEC model shown in Figure 6a is appropriate to fit the corresponding EIS. In Figure 6a, R$_S$ represents the solution resistance, CPE$_c$ and R$_c$ represent the capacitance and resistance of corrosion product, respectively, CPE$_{dl}$ and R$_{ct}$ represent the double layer capacitance and the charge transfer resistance, respectively, R$_L$ represents the inductive resistance, and L represents the inductance. At the same time, for the EIS obtained in the pH 4 to 5 solutions without NaNO$_2$ and in the pH 1 to 5 solutions with NaNO$_2$, only
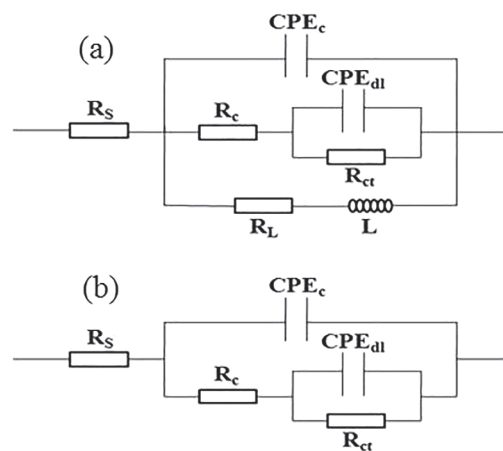

Figure 6. EEC model to fit EIS shown in Figure 5. (a) EIS obtained in the pH 1 to 3 HNO$_3$ solutions without NaNO$_2$ and (b) EIS obtained in the pH 4 and 5 HNO$_3$ solutions without NaNO$_2$ and in the pH 1 to 5 HNO$_3$ solutions with NaNO$_2$.

Table 2. Calculated results of CPE_c, R_c, CPE_{dl} and R_{ct} from the ZVIEW software

pH	Without NaNO$_2$				With NaNO$_2$			
	CPE_c / (F cm^{-2})	R_c / (Ω cm^2)	CPE_{dl} / (F cm^{-2})	R_{ct} / (Ω cm^2)	CPE_c / (F cm^{-2})	R_c / (Ω cm^2)	CPE_{dl} / (F cm^{-2})	R_{ct} / (Ω cm^2)
1	1.32×10^{-4}	12.71	4.94×10^{-4}	18.33	8.76×10^{-4}	0.78	1.59×10^{-3}	1.09
2	1.28×10^{-4}	16.92	2.13×10^{-4}	22.72	7.70×10^{-4}	1.48	1.52×10^{-3}	2.39
3	7.54×10^{-5}	132.87	1.87×10^{-4}	267.70	5.92×10^{-4}	23.01	1.49×10^{-3}	22.51
4	2.74×10^{-5}	172.41	8.74×10^{-5}	963.91	5.80×10^{-4}	21.27	1.17×10^{-3}	96.47
5	1.18×10^{-5}	317.50	7.81×10^{-5}	1083.00	5.61×10^{-4}	32.88	8.93×10^{-4}	356.21

CPE_c: corrosion product capacitance; R_c: corrosion product resistance; CPE_{dl}: double layer capacitance; R_{ct}: charge transfer resistance.
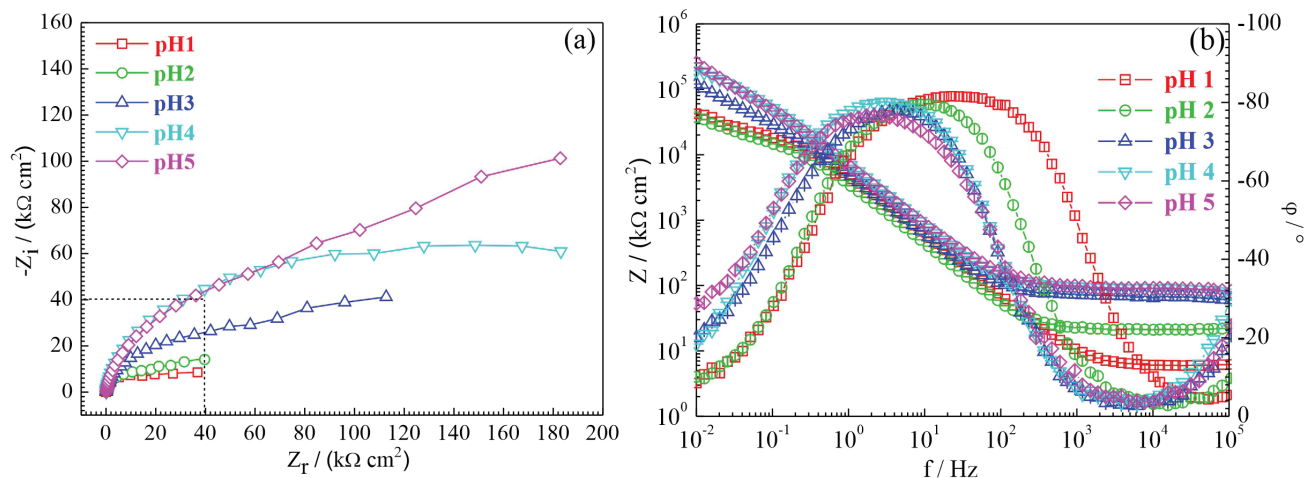
Figure 7. EIS of X65 samples in pH 1 to 5 HNO$_3$ solutions with 0.01 mol L^{-1} NaNO$_2$ at the applied potential of 1.0 V$_{SCE}$: (a) Nyquist plot and (b) Bode plot.

two capacitive semicircles are present, and the EEC model shown in Figure 6b is suitable to fit the corresponding EIS.

Further, the ZVIEW software was applied to analyze the results of EIS. Table 2 lists the calculated results of CPE_c, R_c, CPE_{dl} and R_{ct}.

From Table 2, both in the pH 1 to 5 solutions without NaNO$_2$ and with NaNO$_2$, the values of R_c and R_{ct} increase with the raise of pH value, indicating the decreased corrosion rate.[30] Besides, the values of CPE_c and CPE_{dl} decrease with the raise of pH value, suggesting the decrease of corrosion area on the WE surface.[31] The above results further confirm that the corrosion rate of X65 carbon steel in the high pH solutions is less than that in the low pH solutions, which is in agreement with the results of potentiodynamic polarization curve.

Figure 7 shows the EIS of X65 samples in pH 1 to 5 HNO$_3$ solutions with 0.01 mol L^{-1} NaNO$_2$ at the applied potential of 1.0 V$_{SCE}$. From Figure 4b, for the X65 steel in the pH 1 to 5 solutions with NaNO$_2$, the potential value of 1.0 V$_{SCE}$ is in the passive region; at the same time, comparing Figure 7 with Figure 5, the impedance module at 1.0 V$_{SCE}$ is significantly greater than that at OCP, suggesting the presence of passive film on the surface

of X65 carbon steel.[32] Further, the radius of capacitive semicircle expands obviously with the raise of pH value, indicating the corrosion resistance of passive film formed in the high pH solutions is greater than that formed in the low pH solutions.

From Figure 7b, two points of intersection can be observed on each Bode plot, indicating two time constants. Therefore, the EEC mode shown in Figure 8 is applied to fit the EIS shown in Figure 7, in which CPE_p and R_p represent the capacitance and resistance of passive film, respectively.
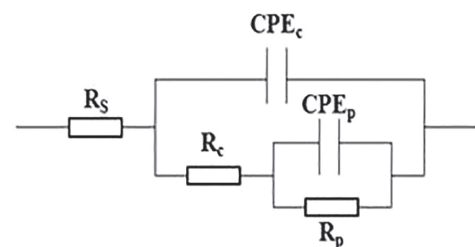

Figure 8. EEC model to fit EIS shown in Figure 7.

Table 3 lists the calculated results of R_p. From Table 3, the R_p value increases gradually with the raise of pH value, which is consistent with the results of E_{trans} and i_{crit} shown

Table 3. Calculated results of R_p from the ZVIEW software

pH	1	2	3	4	5
R_p / (kΩ cm²)	1.52	2.02	6.55	9.64	25.31

R_p: resistance of passive film.

in Table 1. Therefore, it is concluded that for the X65 steel in the pH 1 to 5 solutions with $NaNO_2$, the passivation capability of X65 carbon steel in the high pH solutions is stronger than that in the low pH solutions.[33]

Conclusions

In this work, the influence of 0.01 mol L^{-1} $NaNO_2$ addition in pH 1 to 5 HNO_3 solutions on the corrosion and passivation of X65 carbon steel was investigated and compared. In the pH 1 to 5 solutions without $NaNO_2$, X65 carbon steel presented the electrochemical behavior of activation, and the corrosion rate decreased with the raise of pH value. With the addition of 0.01 mol L^{-1} $NaNO_2$ in pH 1 to 5 HNO_3 solutions, the electrochemical behavior of X65 carbon steel transferred from the active dissolution to the anodic passivation. For the X65 steel in the pH 1 to 5 solutions with $NaNO_2$, with the raise of pH value, the corrosion rate decreased, and the passivation capability strengthened. The corrosion and passivation of X65 carbon steel in pH 1 to 5 HNO_3 solutions without and with 0.01 mol L^{-1} $NaNO_2$ were associated with the cathodic reactions of H^+ reduction, O_2 reduction and NO_2^-/HNO_2 reduction.

Acknowledgments

References

1. Shi, J.; Shi, J. F.; Chen, H. X.; He, Y. B.; Wang, Q. J.; Zhang, Y.; *J. Pressure Vessel Technol.* **2018**, *140*, 031404.

2. Zheng, X. T.; Wu, K. W.; Wang, W.; Yu, J. Y.; Xu, J. M.; Ma, L. W.; *Nucl. Eng. Des.* **2017**, *314*, 285.

3. Feng, B.; Kang, Y. H.; Sun, Y. H.; Yang, Y.; Yan, X. Z.; *Int. J. Appl. Electromagn. Mech.* **2016**, *52*, 357.

4. Huang, H. L.; Tian, J.; *Microelectron. Reliab.* **2017**, *78*, 131.

5. Jiang, S. Y.; Ding, H. Q.; Xu, J.; *J. Tribol.* **2017**, *139*, 014501.

6. Huang, H. L.; Pan, Z. Q.; Qiu, Y. B.; Guo, X. P.; *Microelectron. Reliab.* **2013**, *53*, 1149.

7. Zhong, P.; Ping, K. F.; Qiu, X. H.; Chen, F. X.; *Desalin. Water Treat.* **2017**, *93*, 109.

8. Li, J.; Xiong, C. Y.; Li, J.; Yan, D.; Pu, J.; Chi, B.; Jian, L.; *Int. J. Hydrogen Energy* **2017**, *42*, 16752.

9. Zhou, Y.; Rao, Y. H.; Wang, T. L.; Jens, K. J.; *Int. J. Greenhouse Gas Control* **2018**, *69*, 36.

10. Zhou, Y.; Huang, H. J.; Zhang, P.; Liu, D.; Yan, F. A.; *Surf. Rev. Lett.* **2019**, *26*, 1850218.

11. Deng, F. G.; Wang, L. S.; Zhou, Y.; Gong, X. H.; Zhao, X. P.; Hu, T.; Wu, C. G.; *RSC Adv.* **2017**, *7*, 48876.

12. Xiong, Q. Y.; Zhou, Y.; Xiong, J. P.; *Int. J. Electrochem. Sci.* **2015**, *10*, 8454.

13. Lee, D. Y.; Kim, W. C.; Kim, J. G.; *Corros. Sci.* **2012**, *64*, 105.

14. Dong, Z. H.; Shi, W.; Zhang, G. A.; Guo, X. P.; *Electrochim. Acta* **2011**, *56*, 5890.

15. Dong, Z. H.; Shi, W.; Guo, X. P.; *Corros. Sci.* **2011**, *53*, 1322.

16. Valcarce, M. B.; Vazquez, M.; *Electrochim. Acta* **2008**, *53*, 5007.

17. Reffass, M.; Sabot, R.; Jeannin, M.; Berziou, C.; Refait, P.; *Electrochim. Acta* **2007**, *52*, 7599.

18. Kang, Y. F.; Fang, L. X.; Zhao, Y. H.; Ren, S. Y.; *Math. Probl. Eng.* **2015**, 792069.

19. Zhou, Y.; Zhang, P.; Zuo, Y.; Liu, D.; Yan, F. A.; *J. Braz. Chem. Soc.* **2017**, *28*, 2490.

20. Zhou, Y.; Zuo, Y.; *J. Electrochem. Soc.* **2015**, *162*, C47.

21. Zhou, Y.; Yan, F. A.; *Int. J. Electrochem. Sci.* **2016**, *11*, 3976.

22. Zhou, Y.; Zhang, P.; Huang, H. J.; Xiong, J. P.; Yan, F. A.; *J. Braz. Chem. Soc.* **2019**, *30*, 1688.

23. Zuo, Y.; Yang, L.; Tan, Y. J.; Wang, Y. S.; Zhao, J. M.; *Corros. Sci.* **2017**, *120*, 99.

24. Garces, P.; Saura, P.; Mendez, A.; Zornoza, E.; Andrade, C.; *Corros. Sci.* **2008**, *50*, 498.

25. Cao, C. N.; *Principles of Electrochemistry of Corrosion*; Chemical Industry Press: Beijing, China, 2008.

26. Li, X. J.; Gui, F.; Cong, H. B.; Brossia, C. S.; Frankel, G. S.; *Electrochim. Acta* **2014**, *117*, 299.

27. Pourbaix, M.; *Atlas of Electrochemical Equilibria in Aqueous Solutions*; National Association of Corrosion Engineering: Houston, USA, 1974.

28. Xiong, Q. Y.; Xiong, J. P.; Zhou, Y.; Yan, F. A.; *Int. J. Electrochem. Sci.* **2017**, *12*, 4238.

29. Zhou, Y.; Xiong, J. P.; Yan, F. A.; *Surf. Coat. Technol.* **2017**, *328*, 335.

30. Chen, X.; Xiong, Q. Y.; Feng, Z.; Li, H.; Liu, D.; Xiong, J. P.; Zhou, Y.; *Int. J. Electrochem. Sci.* **2018**, *13*, 1656.

31. Chen, L. C.; Zhang, P.; Xiong, Q. Y.; Zhao, P.; Xiong, J. P.; Zhou, Y.; *Int. J. Electrochem. Sci.* **2019**, *14*, 919.

32. Feng, X. G.; Lu, X. Y.; Zuo, Y.; Zhuang, N.; Chen, D.; *Corros. Sci.* **2016**, *103*, 223.

33. Zhou, Y.; Zhang, P.; Xiong, J. P.; Yan, F. A.; *RSC Adv.* **2019**, *9*, 23589.